Supplementary Information

Direct and Selective Small Molecule Activation of Pro-Apoptotic BAX

Evripidis Gavathiotis[1,2], Denis E. Reyna[1,2], Joseph Bellairs[1], Elizaveta S. Leshchiner, and Loren D. Walensky[1*]

Supplementary Methods

BCL-2 family protein production. Transformed *Escherichia coli* BL21 (DE3) were cultured in ampicillin-containing Luria Broth and protein expression was induced with 0.5 mM isopropyl β-D-1-thiogalactopyranoside (IPTG). The bacterial pellets were resuspended in buffer (20 mM Tris pH 7.2, 250 mM NaCl, complete protease inhibitor tablet), sonicated, and after centifugation at 45,000x*g* for 45 min, the supernatants were applied to glutathione-agarose columns (Sigma) for GST-BCL-X_LΔC, MCL-1ΔNΔC, BFL-1/A1ΔC, and BAKΔC or a chitin column (BioLabs) for Intein-BAX. On-bead digestion of GST-tagged protein was accomplished by overnight incubation at room temperature in the presence of thrombin (75 units) in PBS (3 mL), whereas the intein tag was cleaved from BAX by overnight incubation of the chitin beads at 4°C with 50 mM DTT. BCL-X_LΔC, MCL-1ΔNΔC, BFL-1/A1ΔC, and BAKΔC were purified by size exclusion chromatography (SEC) using 50 mM Tris pH 7.4,150 mM NaCl buffer conditions, and full-length monomeric BAX protein isolated by SEC using a Superdex-75 column (GE Healthcare) and 20 mM HEPES pH 7.2, 150 mM KCl buffer conditions.

Fluorescence polarization binding assays. Direct binding curves were first generated by incubating FITC-BIM SAHB (50 nM) with serial dilutions of full-length BAX, BCL-X_LΔC, MCL-1ΔNΔC, BFL-1/A1ΔC or BAKΔC and fluorescence polarization measured at 20 minutes on a SpectraMax M5 microplate reader (Molecular Devices). For competition assays, a serial dilution of small molecule or acetylated BIM SAHB (Ac-BIM SAHB) was combined with FITC-BIM SAHB (50 nM), followed by the addition of recombinant protein at ~EC_{75} concentration, as determined by the direct binding assay (BAX, BAKΔC: 500 nM; BCL-X_LΔC, MCL-1ΔNΔC, BFL-1/A1ΔC: 200 nM). Fluorescence polarization was measured at 20 minutes and IC_{50} values calculated by nonlinear regression analysis of competitive binding curves using Prism software (Graphpad).

NMR samples and spectroscopy. Protein samples were prepared in 25 mM sodium phosphate, 50 mM NaCl solution at pH 6.0 in 5% D_2O. **BAM7** or **ANA-BAM16** (10 mM stock) was titrated into a solution of 50 μM BAX or BAX Lys21Glu to achieve the indicated molar ratios. Correlation ^1H-^{15}N HSQC spectra[1] were acquired at 25°C on a Bruker 800 MHz NMR spectrometer equipped with a cryogenic probe, processed using NMRPipe[2], and analyzed with

NMRView[3]. The weighted average chemical shift difference Δ at the indicated molar ratio was calculated as $\sqrt{\left\{(\Delta H)^2 + (\Delta N/5)^2\right\}/2}$ in p.p.m. The absence of a bar indicates no chemical shift difference, or the presence of a proline or residue that is overlapped or not assigned. BAX cross-peak assignments were applied as previously reported[4]. The significance threshold for backbone amide chemical shift changes was calculated based on the average chemical shift across all residues plus the standard deviation, in accordance with standard methods[5].

Stapled peptide and small molecule ligands. BIM SAHBs were synthesized, purified, and characterized as reported[6,7]. SAHBs were isolated by LC-MS at >95% purity and quantitated by amino acid analysis. BIM SAHB composition and LC-MS profiles are presented in **Supplementary Figures 3a, 3c**. **BAM7** and ANA-BAMs 1-16 were purchased from ChemBridge (>90% purity). NMR analysis of **BAM7** (ChemBridge, #5258079) documented a 2-ethoxy rather than 4-ethoxy composition. The molecular identity and activity of **BAM7** was then reconfirmed by repeat synthesis (CreaGen Biosciences), NMR, MS, and binding analyses (**Fig. 1c, Supplementary Fig. 4**, **Methods**).

BAX oligomerization assay. BAM7 or **ANA-BAM16** was added to a 200 μL solution (20 mM HEPES/KOH pH 7.2, 150 mM KCl, 0.5% CHAPS) containing size exclusion chromatography (SEC)-purified, monomeric BAX or BAX Lys21Glu (5 μM) at the indicated protein:compound ratios. The mixtures and BAX monomer alone were incubated at 30°C for the indicated durations and then subjected to analysis by SEC using an SD75 column and 20 mM HEPES/KOH pH 7.2, 150 mM KCl running buffer. The monomeric and oligomeric fractions elute at ~11.5-12.0 min (23-24 mL) and ~6.5-7.5 min (14-15 mL), respectively. Protein standards (GE Healthcare) were used to calibrate the molecular weights of gel filtration peaks. Replicates were performed using at least two independent preparations of freshly SEC-purified monomeric BAX protein. Protein fractions were further subjected to mass spectrometry to monitor for co-elution of associated small molecule.

Liposomal release assay. Liposomes were composed of the following molar percentages of lipids (Avanti Polar Lipids): phosphatidylcholine, 48%; phosphatidylethanolamine, 28%; phosphatidylinositol, 10%; dioleoyl phosphatidylserine, 10%; and tetraoleoyl cardiolipin, 4% and were loaded with ANTS/DPX (Molecular Probe) upon extrusion. BAX or BAX Lys21Glu (400 nM) was combined with **BAM7** or **ANA-BAM16** at the indicated protein:compound ratios in 96-well format (Corning) and then liposomes were added (10 μL from 50 μM total lipid stock) in assay buffer (10 mM HEPES pH 7, 200 mM KCl, 5 mM $MgCl_2$, and 0.2 mM EDTA) to a final volume of 100 μl. Liposomal release was quantified based on the increase in fluorescence that occurs when the ANTS fluorophore is separated from the DPX quencher upon release from the liposomes into the supernatant. Fluorescence (λ_{ex} = 355 nm and λ_{em} = 520 nM) was measured over time at 30°C using a Tecan Infinite M1000 plate reader.

Maximal ligand-induced BAX-mediated release was determined by treating liposomes with a mixture of tBID (30 nM) and BAX (400 nM). The percentage release of ANTS/DPX at 90 min was calculated as percentage release = $((F - F_0)/(F_{100} - F_0)) \times 100$, where F_0 and F_{100} are baseline and maximal fluorescence, respectively.

BAX translocation assay. MEFs were seeded on uncoated 24-well glass bottom plates at a density of $2.5x10^5$ cells/well in 500 μL of supplemented DMEM. After 6 h, cells were transfected using Lipofectamine™ 2000 (Invitrogen) according to the manufacturer's protocol, using 750 ng of plasmid DNA and 1.0 μL of Lipofectamine™ per well. Plasmid DNA was generated by cloning full-length BAX into the pEGFP-C3 plasmid (Clontech) using 5' PstI and 3' XbaI restriction sites. After overnight transfection, cells were treated with the indicated concentrations of **BAM7** or vehicle (0.3% DMSO) in supplemented DMEM for 6 hours. Mitochondria were labeled with MitoTracker® Red CMXRos (Invitrogen) according to the manufacturer's protocol using 20 nM probe in 500 μL supplemented, phenol red-free DMEM for 15 min. The cells were then incubated in fresh media for an additional 15 min prior to imaging. Confocal microscopy was performed using a Yokogawa spinning disk confocal microscope (Yokogawa Electric Corporation) equipped with a Nikon inverted Ti microscope. Solid state lasers set at 488 nm and 561 nm were used to visualize EGFP and MitoTracker® Red CMXRos, respectively. The plate temperature was maintained at 37°C using an In Vivo environmental chamber (In Vivo Scientific). Images were collected using an Andor iXon DU-897 EM-CCD camera (Andor Technology) and analyzed with ImageJ software (NIH). Percent EGFP-positive cells was determined by counting EGFP-positive and Mitotracker-positive cells. Percent BAX translocation was calculated by dividing the number of cells containing mitochondrion-localized BAX by the total number of EGFP-positive cells. Each treatment was performed in quadruplicate with >200 cells counted per well.

Light microscopy. MEFs ($5x10^3$ cells/well) were plated for 24 hours on glass bottom culture dishes (MatTek Corp., MA) and then incubated with **BAM7** (15 μM) or vehicle (0.15% DMSO). Live cell imaging was performed using a TE2000-E2 Nikon microscopy equipped with a temperature and CO_2-controlled chamber that maintained an atmosphere of 3-5% humidified CO_2 at 37°C. A Hamamatsu Orca ER digital CCD camera was used to capture images at 20x magnification for 24 hours at 20 min intervals. Acquisition, hardware control, and image analysis was performed using Nikon NIS-Elements software.

Supplementary Results

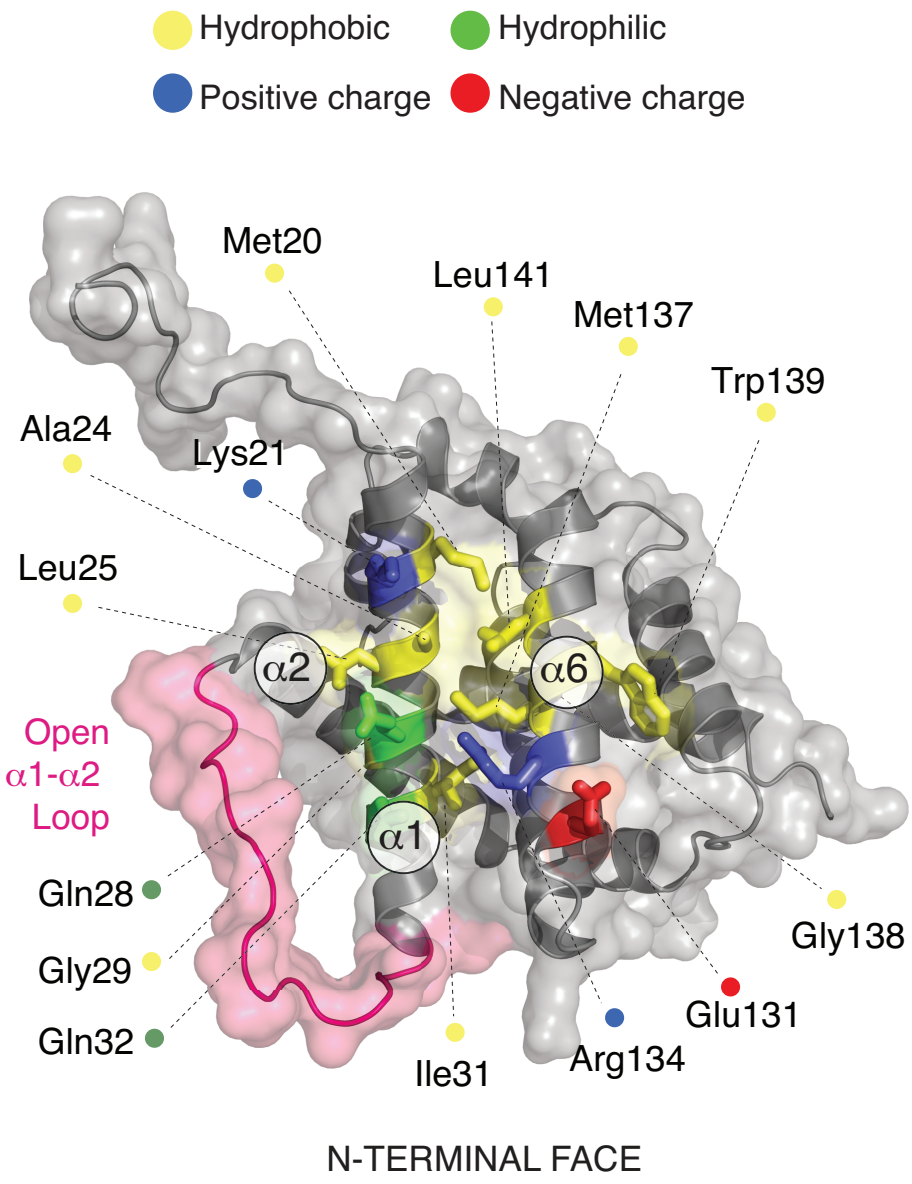

Supplementary Figure 1. Structural features of the BAX activation site. The BH3 trigger site is comprised of a hydrophobic groove with a perimeter of charged and hydrophilic residues from α-helices 1 and 6. BAX is oriented to demonstrate its N-terminal face and the individual amino acids that comprise the trigger site, with the unstructured loop (pink) between α1 and α2 depicted in the open position.

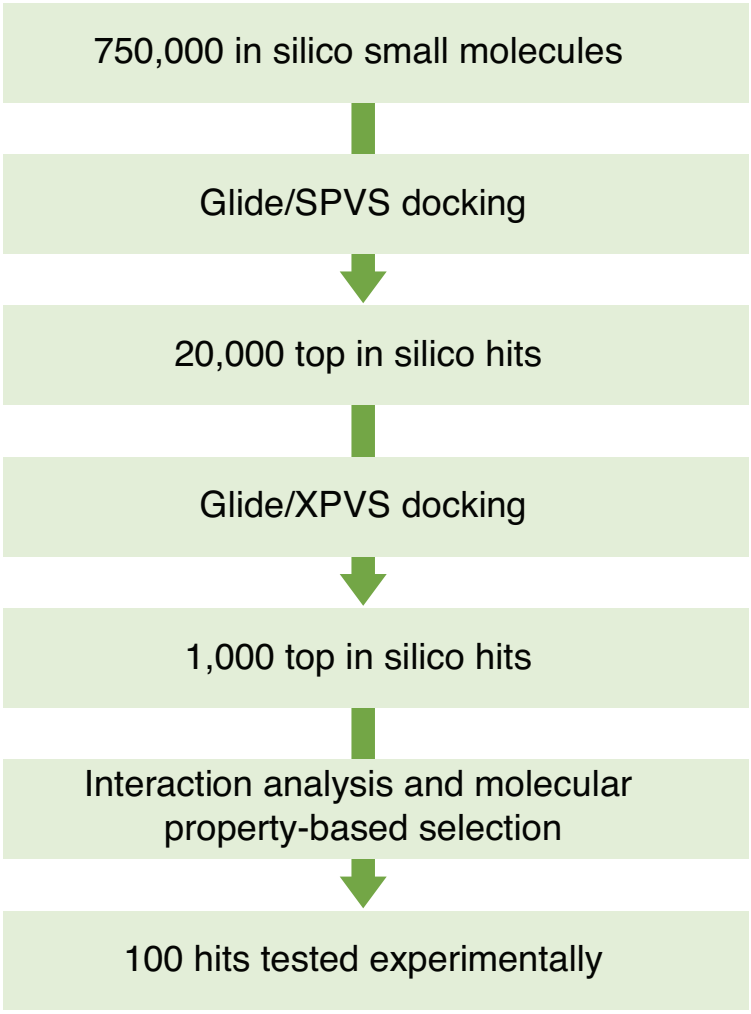

Supplementary Figure 2. *In silico* screen for BAX activator molecules (BAMs). A computational screening algorithm employing an *in silico* library of 750,000 small molecules docked on averaged minimized BAX structures yielded a panel of 100 candidate BAX activator molecules (BAMs).

Nature Chemical Biology: doi:10.1038/nchembio.995

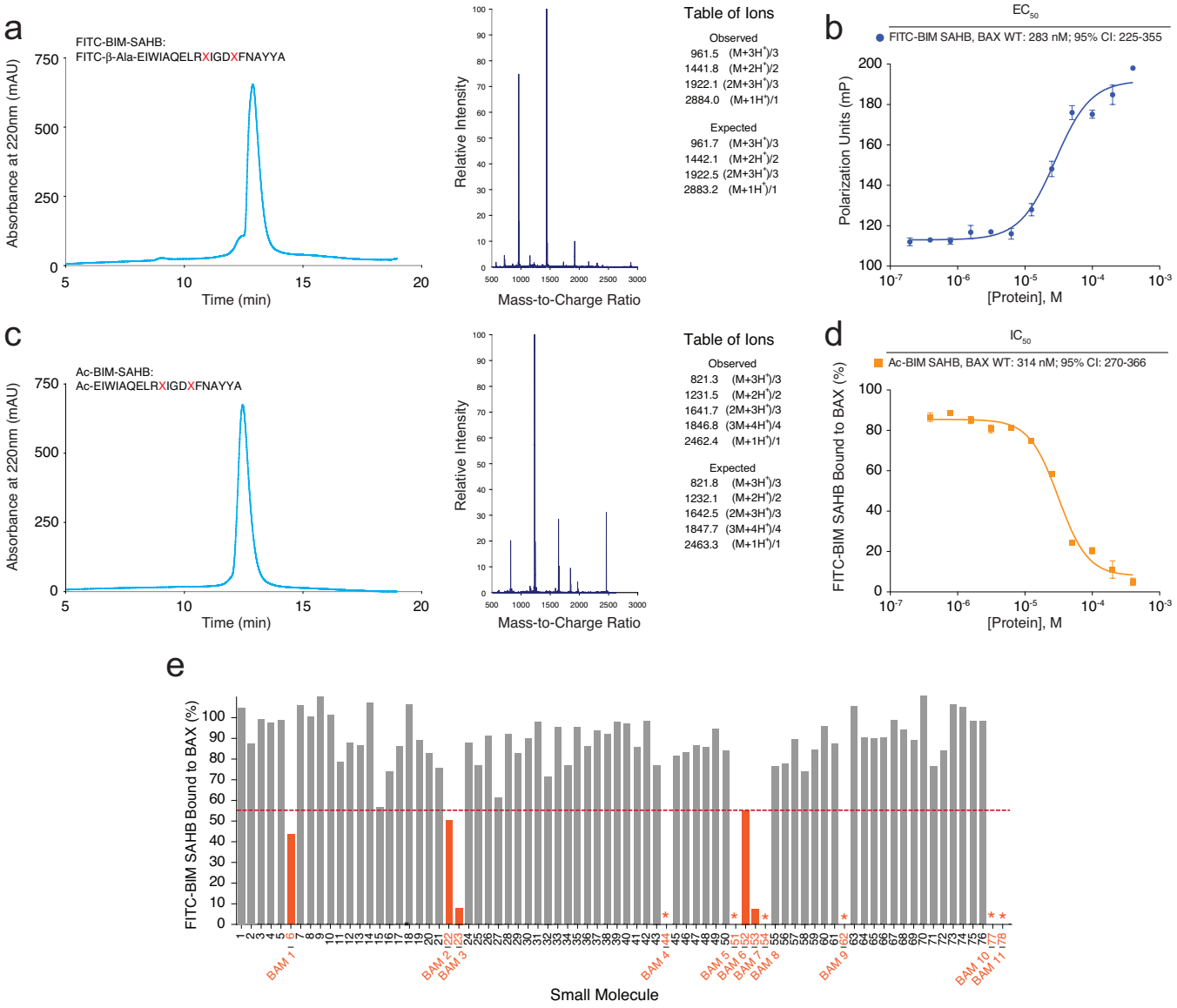

Supplementary Figure 3. Competitive binding activity of BAX activator molecules (BAMs). (**a**) Amino acid sequence, purification, and characterization of FITC-BIM SAHB. X, stapling amino acid (**b**) The direct binding interaction between FITC-BIM SAHB and recombinant full-length BAX formed the basis for developing a competitive fluorescence polarization binding assay to screen for BAMs. (**c**) Amino acid sequence, purification, and characterization of N-terminal acetylated BIM SAHB (Ac-BIM SAHB). X, stapling amino acid (**d**) Ac-BIM SAHB, which effectively competed with FITC-BIM SAHB for BAX binding, served as a positive control for the assay. (**e**) Eleven molecules achieved >55% displacement of FITC-BIM SAHB at the 100 M screening dose and were advanced to dose-responsive competitive binding analysis. *, no detectable FITC-BIM SAHB binding

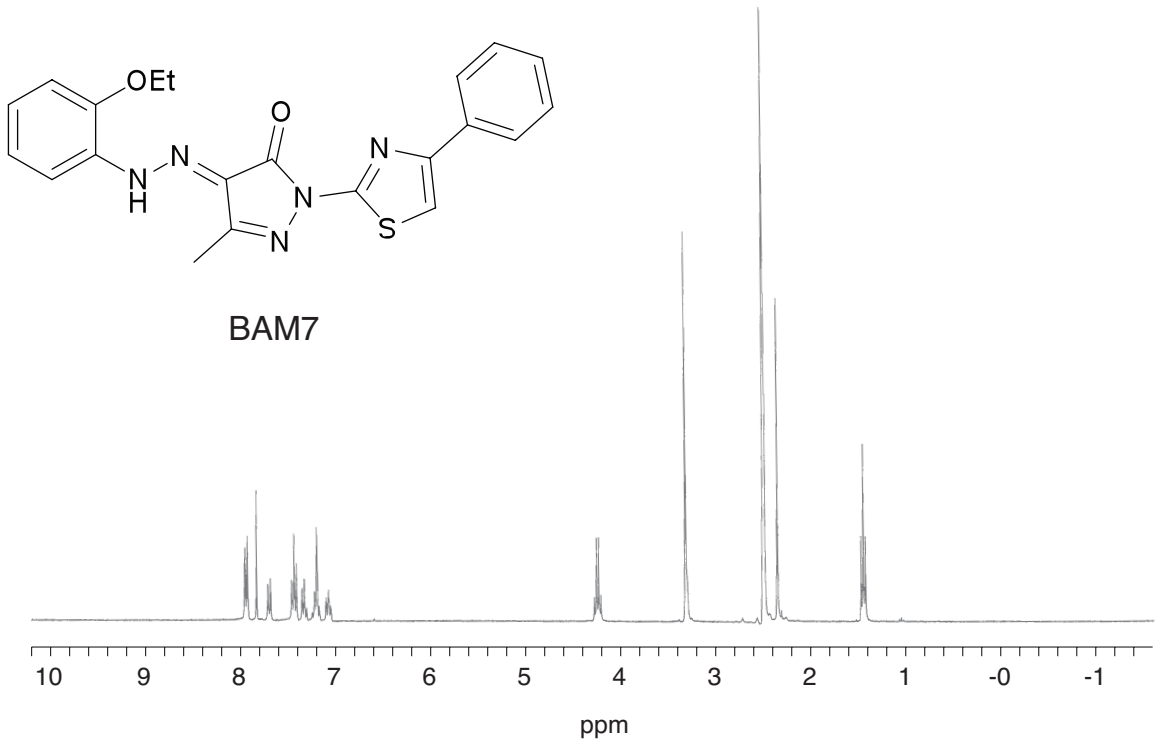

Supplementary Figure 4. ^{1}H-NMR spectrum of **BAM7**.

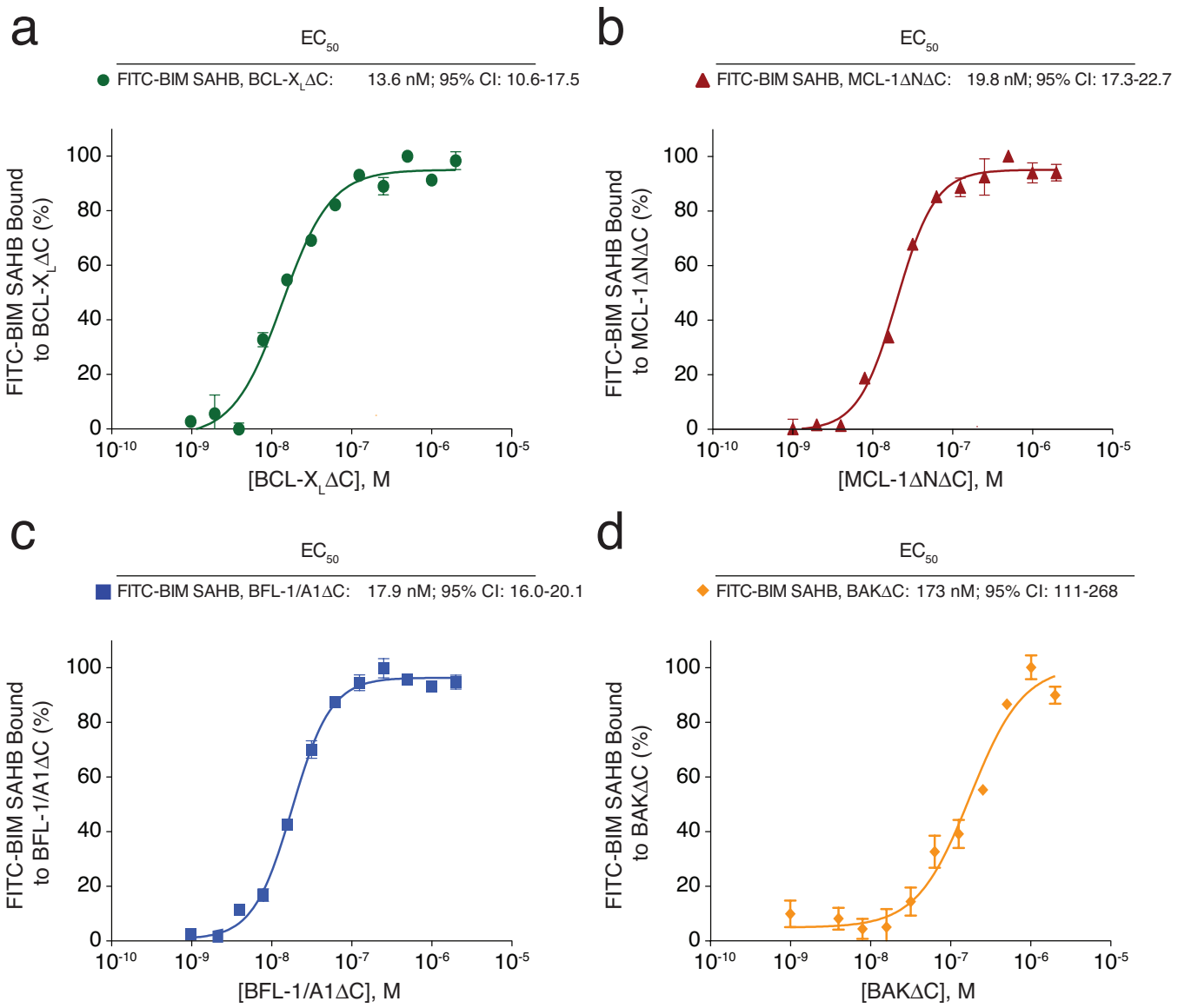

Supplementary Figure 5. BIM SAHB binds to a broad range of BCL-2 family targets. Direct binding isotherms are shown for engagement of FITC-BIM SAHB by BCL-X_LΔC, MCL-1ΔNΔC, BFL-1/A1ΔC and BAKΔC, as measured by FPA.

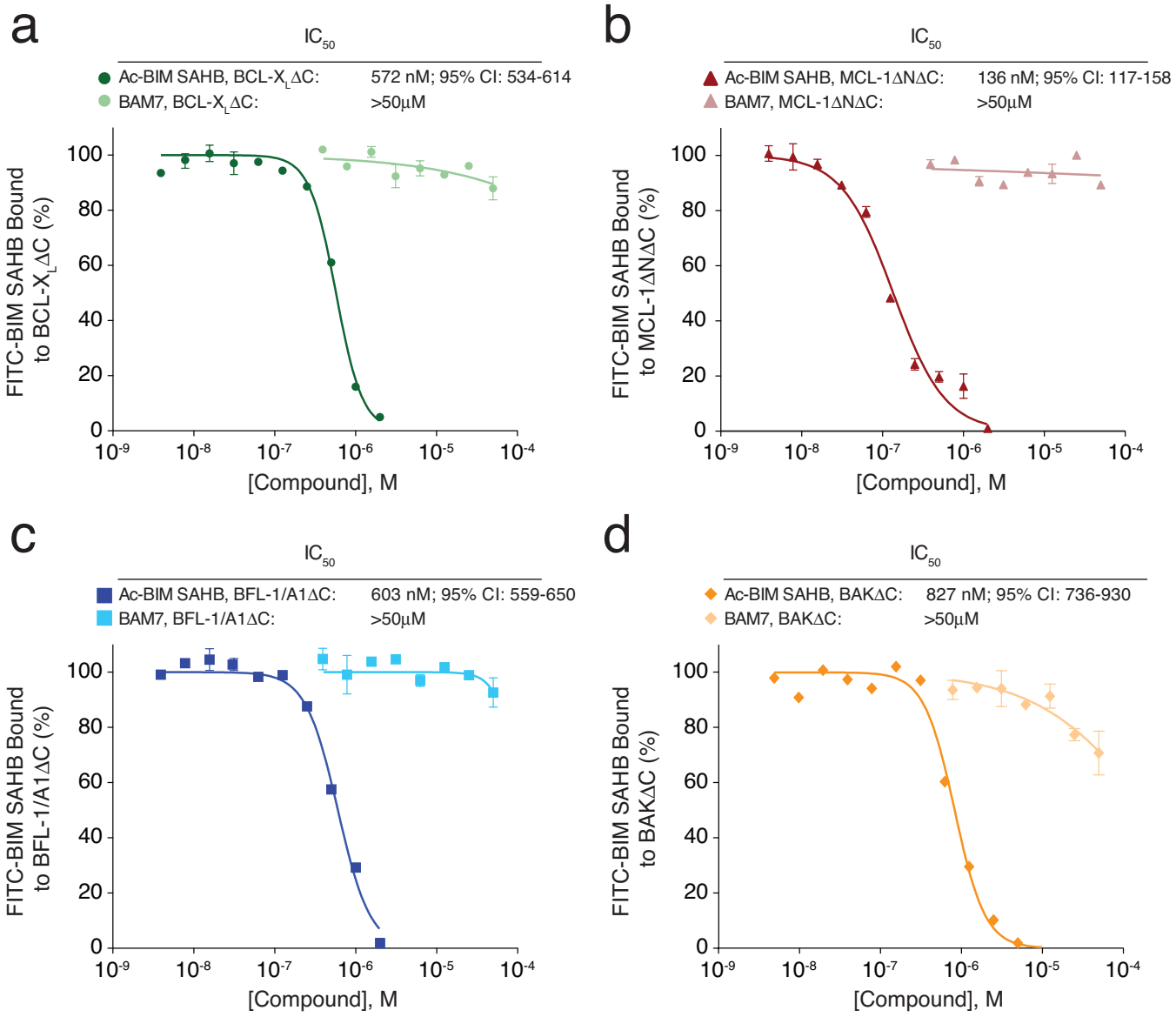

Supplementary Figure 6. Specificity of **BAM7** for pro-apoptotic BAX. The specificity of **BAM7** for the BH3 binding site on BAX was examined by competitive FPA employing FITC-BIM SAHB and (**a**) BCL-X_L C, (**b**) MCL-1 N C, (**c**) BFL-1/A1 C, and (**d**) BAK C. Whereas Ac-BIM SAHB effectively competed with FITC-BIM SAHB for binding to the diversity of BCL-2 family multidomain proteins, **BAM7** demonstrated little to no capacity to compete with FITC-BIM SAHB for interaction at the BH3 binding sites of BCL-X_L C, MCL-1 N C, BFL-1/A1 C, or BAK C. Data are mean and s.d. for experiments performed in at least triplicate.

Nature Chemical Biology: doi:10.1038/nchembio.995

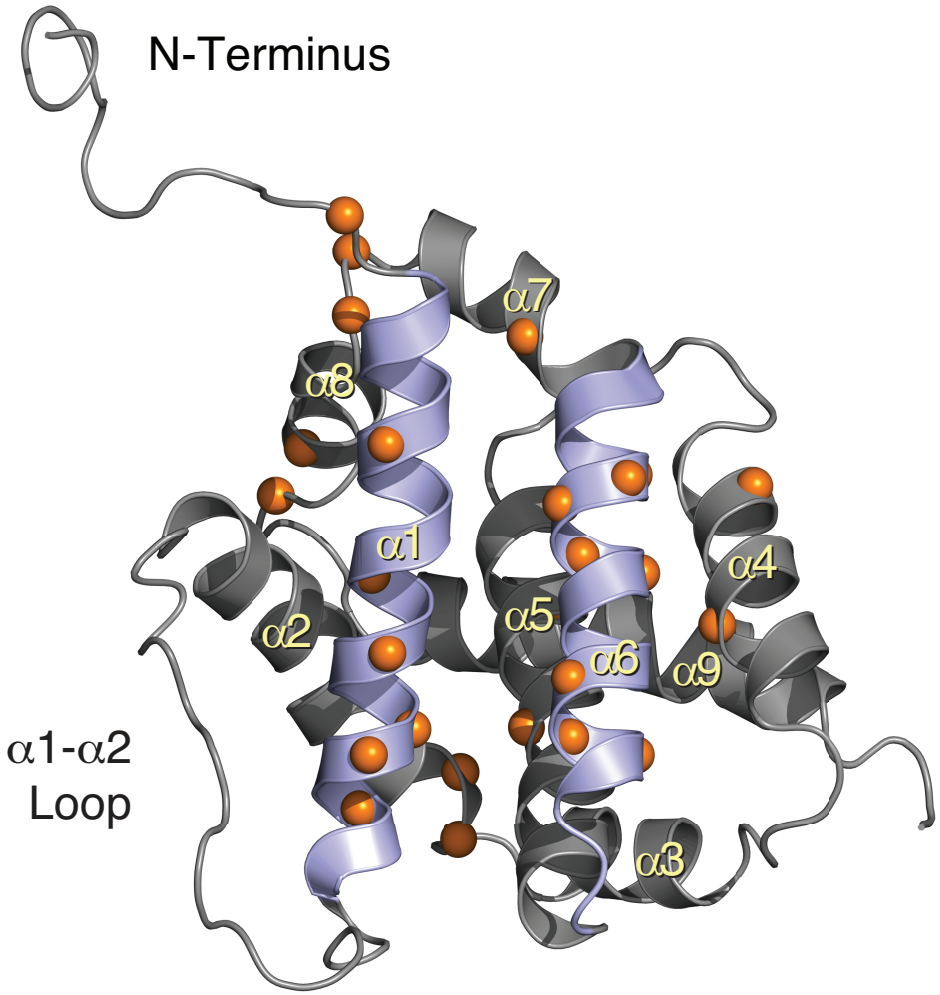

Supplementary Figure 7. BAM7 directly engages the BAX trigger site. Measured chemical shift changes of ^{15}N-BAX upon **BAM7** titration up to a ratio of 1:1 BAX:**BAM7** are concentrated in the region of the trigger site (α1, α6; magenta). Cα atoms of affected residues are represented as orange spheres in the ribbon diagram and orange bars in the plot (calculated significance threshold >0.009 p.p.m.).

Nature Chemical Biology: doi:10.1038/nchembio.995

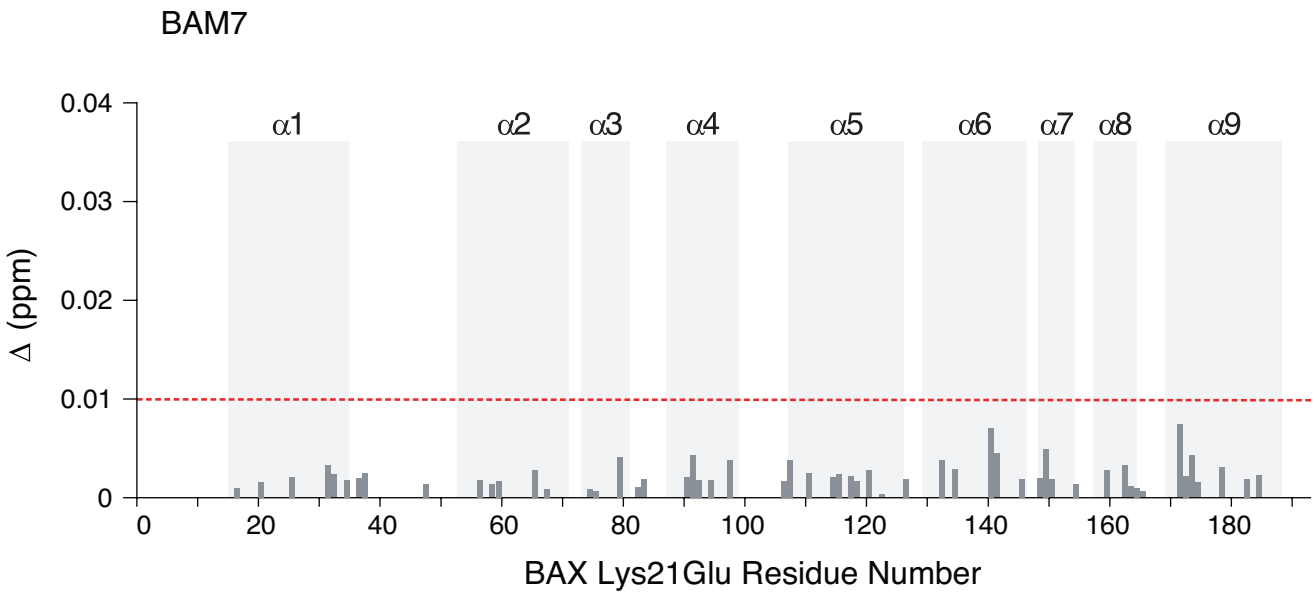

Supplementary Figure 8. Lys21Glu mutagenesis abrogates the **BAM7**/BAX interaction as determined by NMR analysis of ^{15}N-BAX Lys21Glu upon **BAM7** titration up to a 2:1 **BAM7**:^{15}N-BAX Lys21Glu ratio.

Nature Chemical Biology: doi:10.1038/nchembio.995

a

Analogue of BAM7 (ANA-BAM)	Structure	FITC-BIM SAHB Bound to BAX (%) at 50 μM	R1 Benzyl Group	R2 Benzyl Group
1	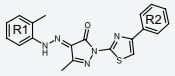	44	2-methyl	
2	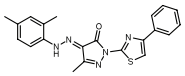	47	2,4-dimethyl	
3	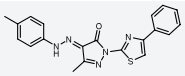	47	4-methyl	
4	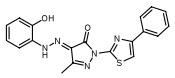	47	2-hydroxyl	
5	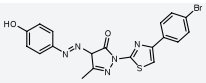	51	4-hydroxyl	4-bromo
6	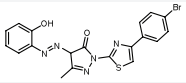	53	2-hydroxyl	4-bromo
7	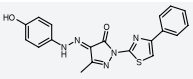	59	4-hydroxyl	
8	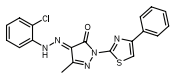	60	2-chloro	
9	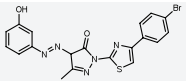	60	3-hydroxyl	4-bromo
10	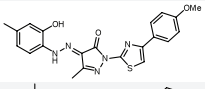	60	2-hydroxy-4-methyl	4-methoxy
11	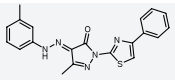	61	3-methyl	
12	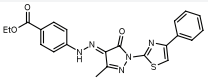	61	4-ethyl ester	
13	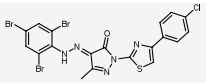	67	2,4,6-tribromo	4-chloro
14	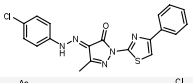	68	4-chloro	
15	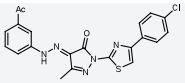	72	3-acetyl	4-chloro
16	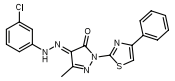	77	3-chloro	

b

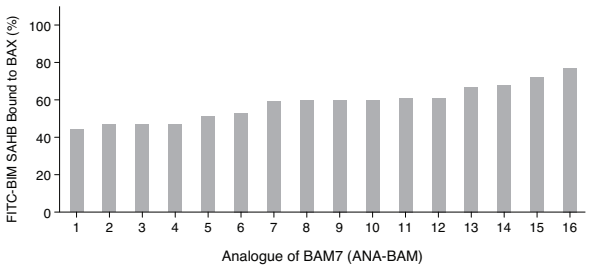

Supplementary Figure 9. (**a**, **b**) A series of analogues of **BAM7** (ANA-BAMs) with alternative derivatizations at the phenylhydrazono and phenylthiazole side groups manifest differential BAX binding activity, with **ANA-BAM16** exhibiting the most impaired binding profile by competitive FPA screening.

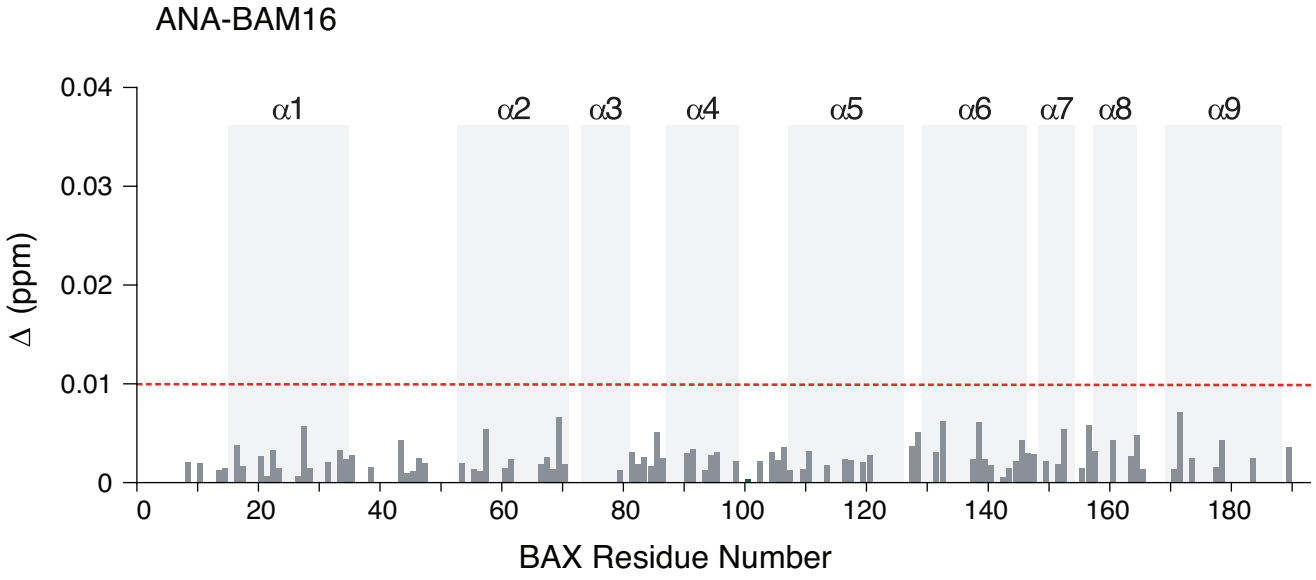

Supplementary Figure 10. Alternative derivatization of the phenylhydrazono moiety of **BAM7** markedly impairs the BAX interaction, as determined by NMR analysis of ^{15}N-BAX upon **ANA-BAM16** titration up to a 2:1 **ANA-BAM16**:^{15}N- BAX ratio.

Nature Chemical Biology: doi:10.1038/nchembio.995

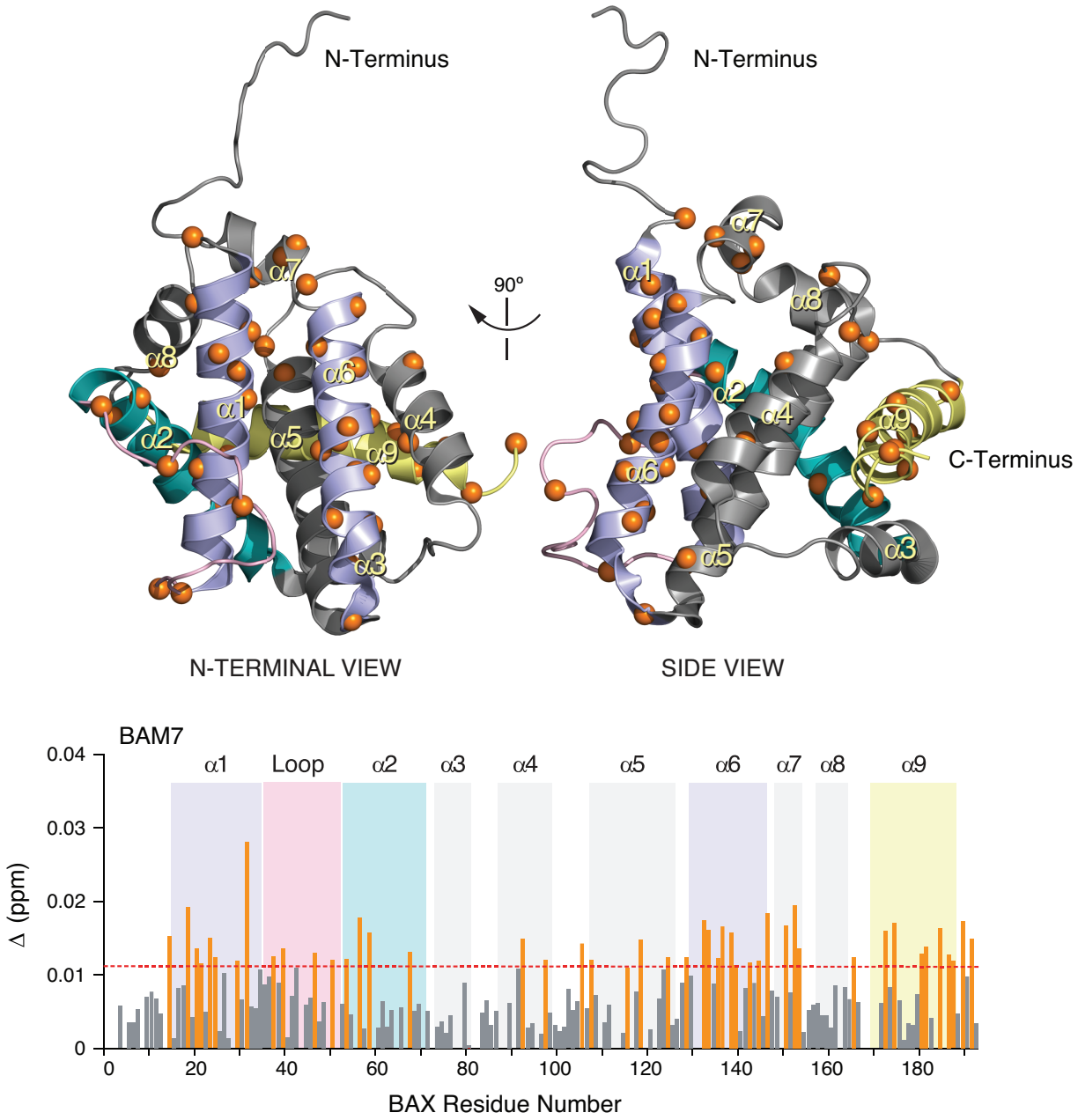

Supplementary Figure 11. BAM7 induces allosteric changes in key functional domains implicated in functional BAX activation. Upon increasing the ratio of **BAM7**:^{15}N-BAX from 1:1 to 2:1, a series of chemical shift changes become more prominent in the α1-α2 loop, α2 (BH3), and α9, three regions previously implicated in BIM BH3-triggered N-terminal loop opening, BAX BH3 exposure, and C-terminal helix mobilization, respectively[8]. These **BAM7**-induced allosteric changes reflect a major conformational change that has been linked to functional BAX activation. Cα atoms of affected residues are represented as orange spheres in the ribbon diagram and orange bars in the plot (calculated significance threshold >0.011 p.p.m.). The α1-α2 loop, α2 (BH3), and α9 are highlighted in pink, cyan, and yellow, respectively.

Nature Chemical Biology: doi:10.1038/nchembio.995

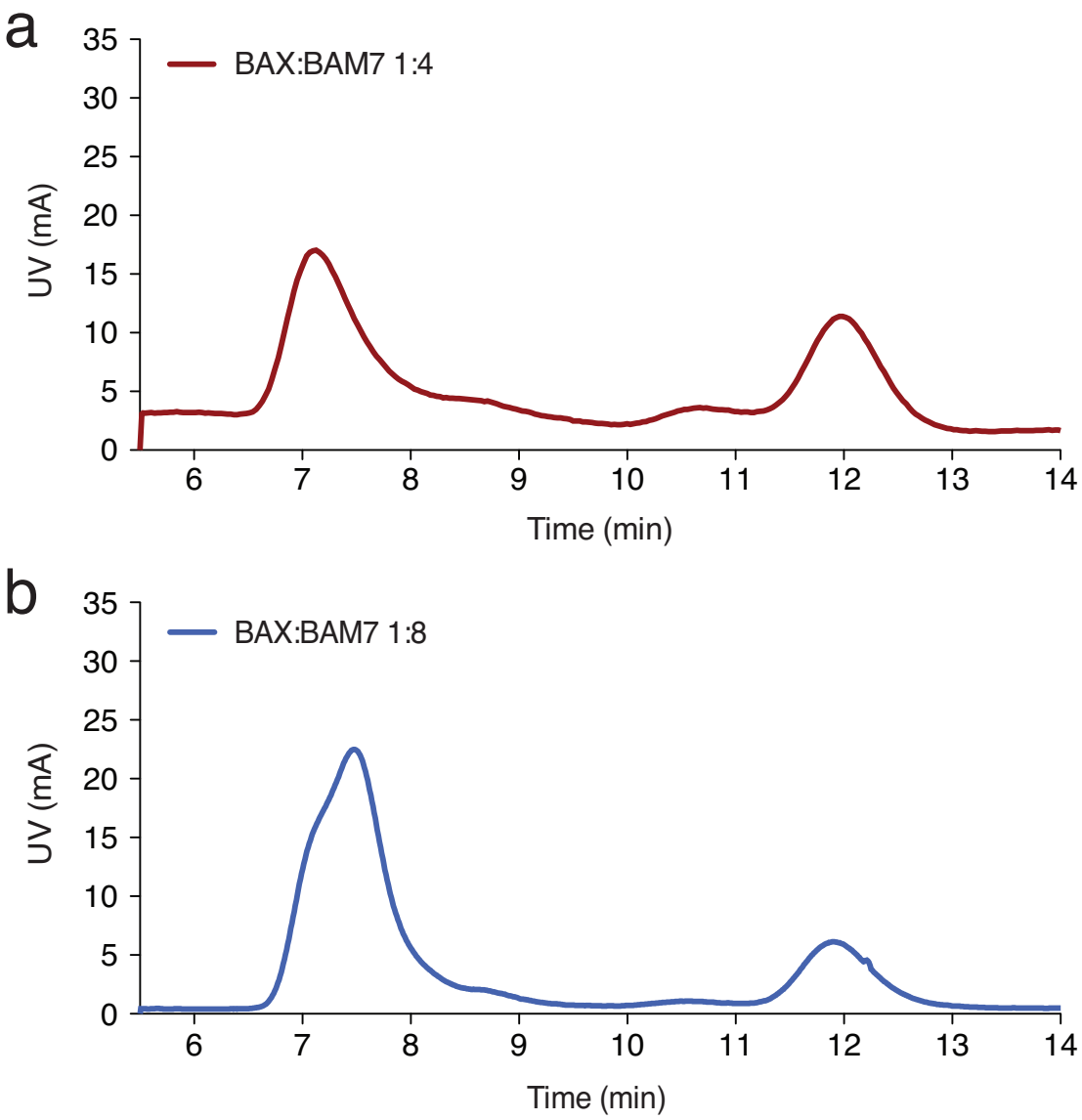

Supplementary Figure 12. BAM7-induced BAX oligomerization. Incubation of wild-type BAX with **BAM7** in solution at 1:4 and 1:8 BAX:**BAM7** dose ratios dose-responsively triggers conversion of monomeric BAX to an oligomeric species, as detected by SEC analysis.

Nature Chemical Biology: doi:10.1038/nchembio.995

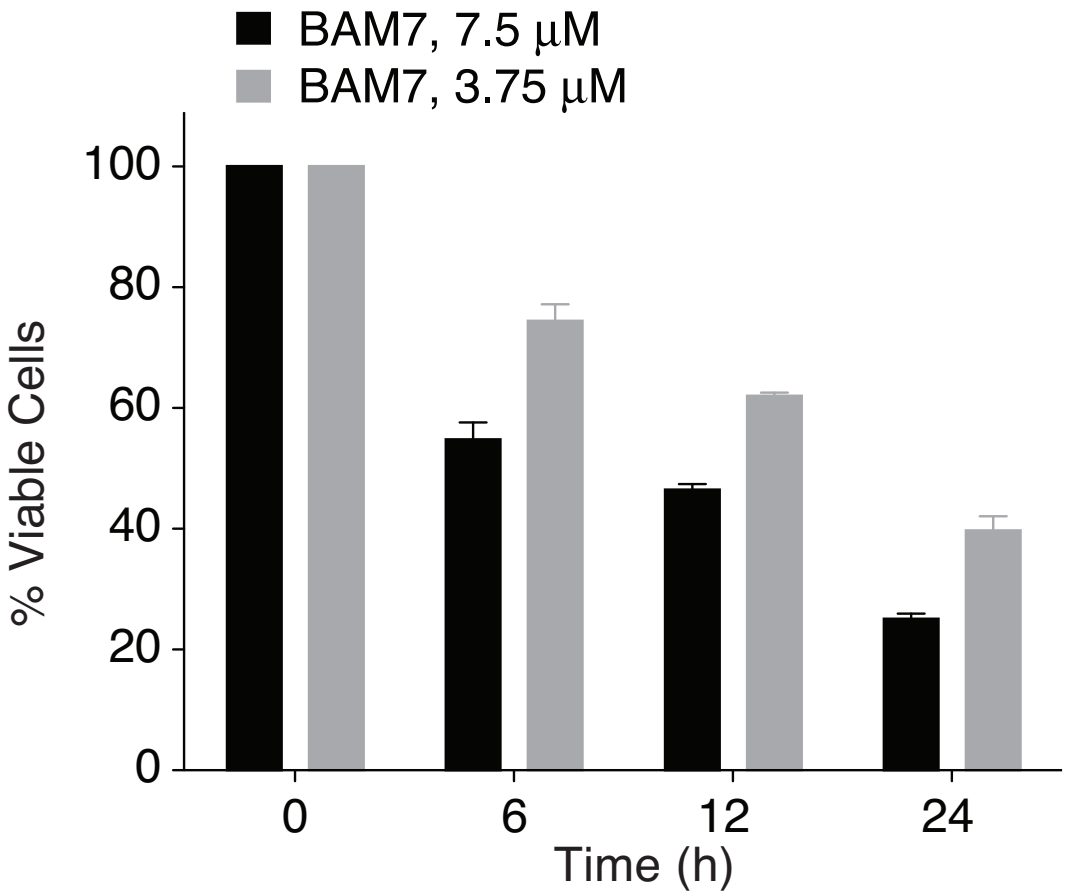

Supplementary Figure 13. BAM7 impairs the viability of *Bak*$^{-/-}$ MEFs in a time-responsive manner. The experiment was performed using an independent aliquot of *Bak*$^{-/-}$ MEFs and lot of **BAM7**.

Nature Chemical Biology: doi:10.1038/nchembio.995

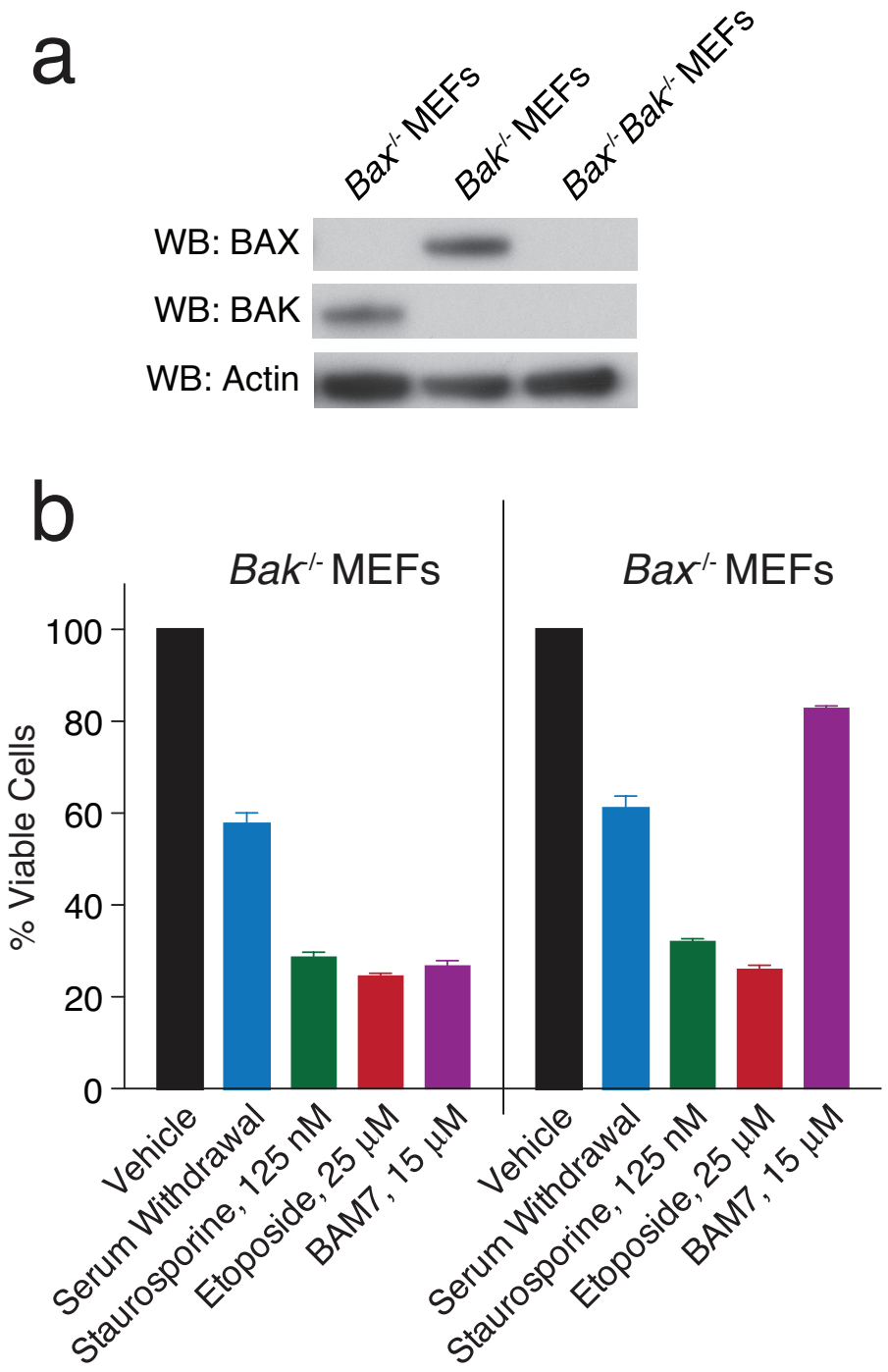

Supplementary Figure 14. Selective activity of **BAM7** in *Bak*$^{-/-}$ MEFs. (**a**) Western analysis of genetically-defined mouse embryonic fibroblasts (MEFs) document that *Bak*$^{-/-}$ MEFs express BAX but not BAK, *Bax*$^{-/-}$ MEFs express BAK but not BAX, and *Bax*$^{-/-}$*Bak*$^{-/-}$ MEFs express neither BAX nor BAK. (**b**) Standard pro-apoptotic stimuli, such as serum withdrawal (48 h), staurosporine (24 h), and etoposide (24 h), elicited an equivalent cytotoxic response in *Bax*$^{-/-}$ and *Bak*$^{-/-}$ MEFs, whereas **BAM7** (24 h) selectively impaired the viability of *Bak*$^{-/-}$ MEFs.

Nature Chemical Biology: doi:10.1038/nchembio.995

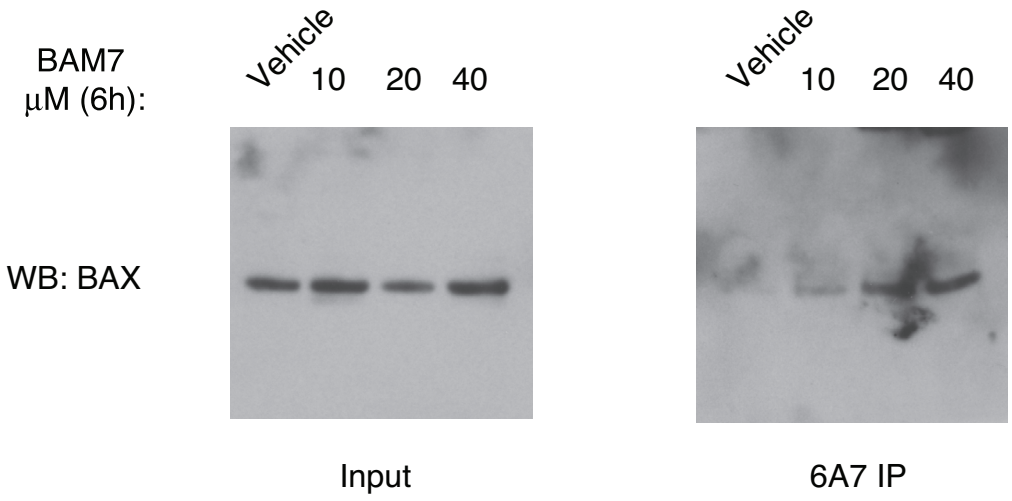

Supplementary Figure 15. BAM7-induced BAX 6A7 epitope exposure (full blots). **BAM7** treatment of *Bak*$^{-/-}$ MEFs resulted in dose-responsive exposure of the N-terminal BAX activation epitope, as captured by 6A7 immunoprecipitation from the corresponding cellular lysates.

Nature Chemical Biology: doi:10.1038/nchembio.995

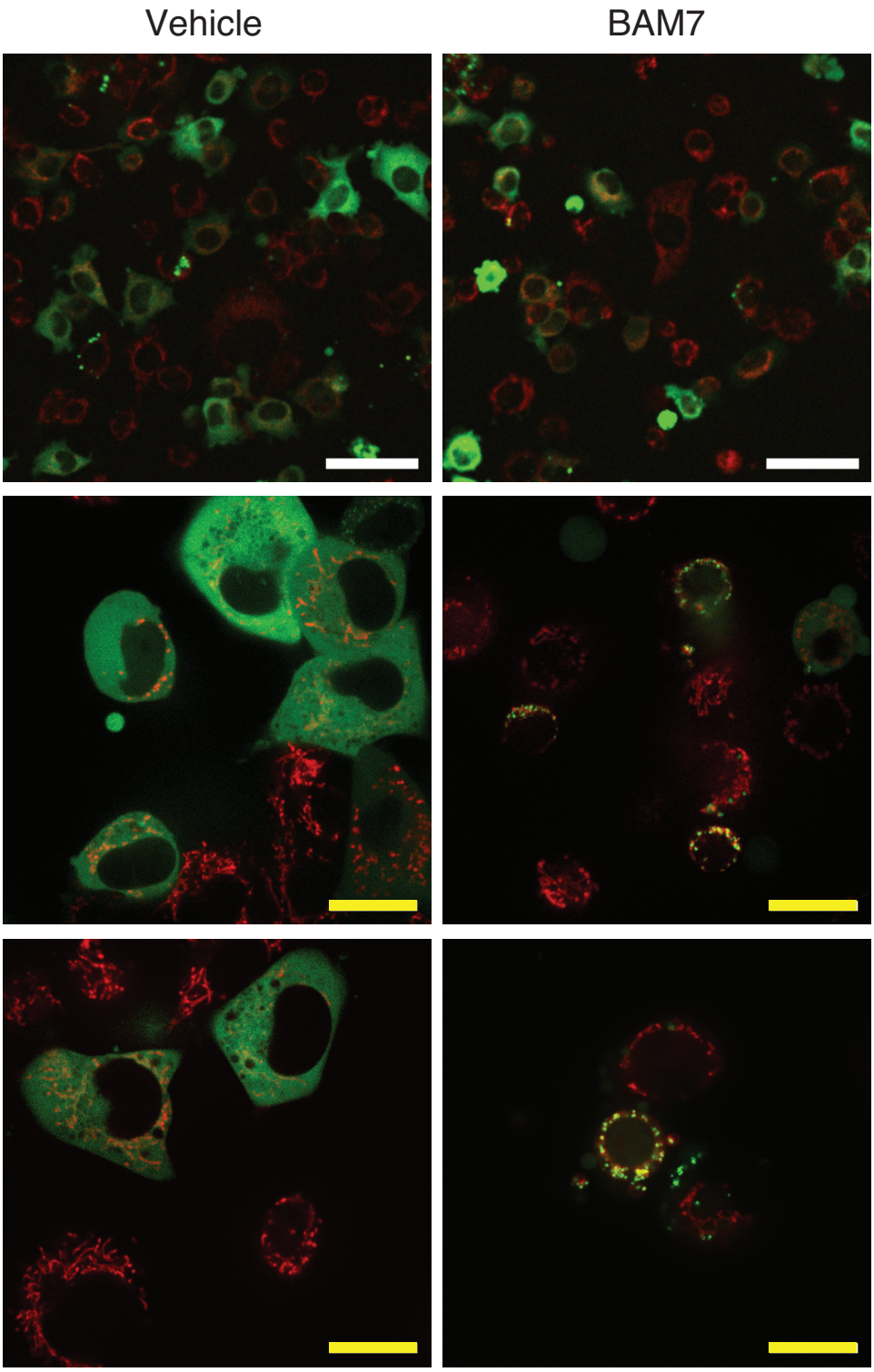

Supplementary Figure 16. BAM7-induced BAX translocation to mitochondria. *Bax*$^{-/-}$*Bak*$^{-/-}$ MEFs reconstituted with EGFP-BAX (~60% EGFP-positive cells) displayed dose-responsive BAX translocation upon exposure to **BAM7**, as evidenced by the conversion of EGFP-BAX localization from a diffuse pattern to a mitochondrion-localized distribution. EGFP-BAX, green; Mitotracker, red; Colocalization, yellow; **BAM7**, 30 M; Vehicle, 0.3% DMSO; t, 6h. White bar, 50 microns; yellow bar, 15 microns

Nature Chemical Biology: doi:10.1038/nchembio.995

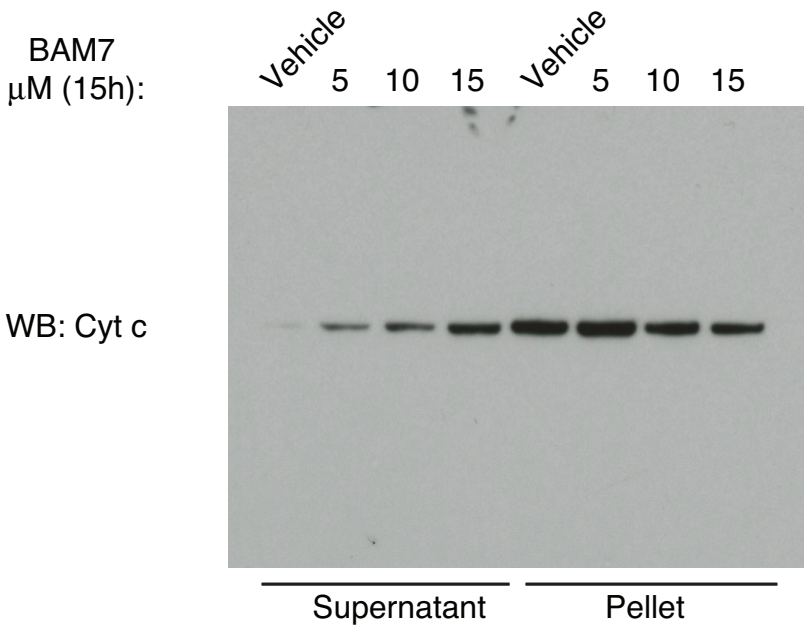

Supplementary Figure 17. BAM7-induced cytochrome c release (full blots). **BAM7** treatment of *Bak*$^{-/-}$ MEFs elicited dose-responsive mitochondrial cytochrome *c* release, as monitored by western analysis of the supernatant and pellet fractions.

Nature Chemical Biology: doi:10.1038/nchembio.995

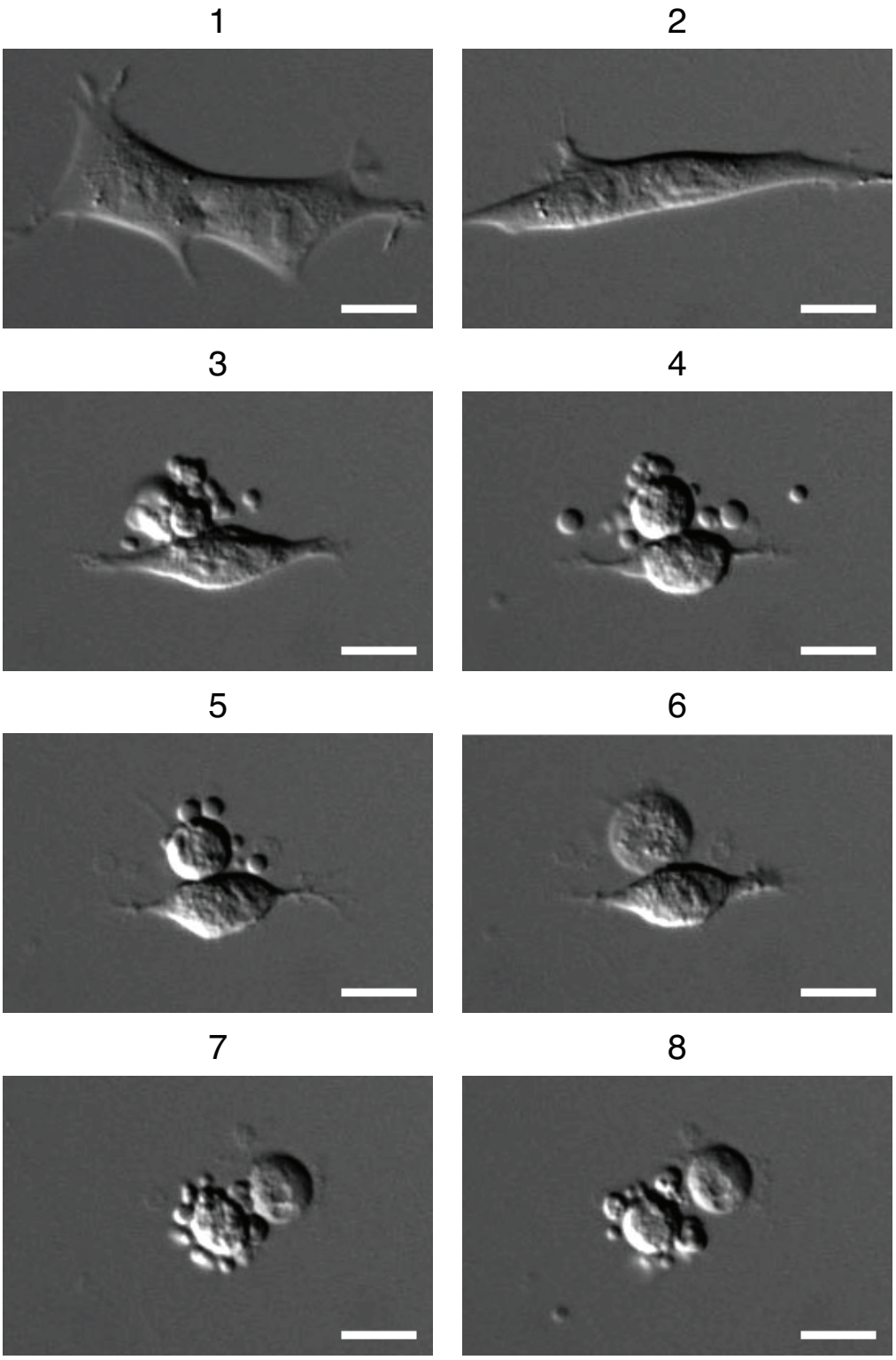

Supplementary Figure 18. Apoptosis morphology of **BAM7**-treated *Bak*$^{-/-}$ MEFs. *Bak*$^{-/-}$ MEFs demonstrate the morphologic features of apoptosis in response to **BAM7** treatment (15 M). The time lapse images reveal progressive cellular shrinkage, membrane blebbing, and the formation of apoptotic bodies. 1, 20 min; 2, 6 h; 3, 12 h; 4, 12.5 h; 5, 13.5 h, 6, 14.5 h; 7, 16.5 h; 8, 17.5 h. White bar, 15 microns

Nature Chemical Biology: doi:10.1038/nchembio.995

Supplementary References

1. Grzesiek, S. & Bax, A. The importance of not saturating water in protein NMR: application to sensitivity enhancement and NOE measurements. *J Am Chem Soc* **115**, 12593-12594 (1993).
2. Delaglio, F. et al. NMRPipe: a multidimensional spectral processing system based on UNIX pipes. *J Biomol NMR* **6**, 277-93 (1995).
3. Johnson, B.A. Using NMRView to visualize and analyze the NMR spectra of macromolecules. *Methods Mol Biol* **278**, 313-52 (2004).
4. Suzuki, M., Youle, R.J. & Tjandra, N. Structure of Bax: coregulation of dimer formation and intracellular localization. *Cell* **103**, 645-54 (2000).
5. Marintchev, A., Frueh, D. & Wagner, G. NMR methods for studying protein-protein interactions involved in translation initiation. *Methods Enzymol* **430**, 283-331 (2007).
6. Bird, G.H., Bernal, F., Pitter, K. & Walensky, L.D. Synthesis and biophysical characterization of stabilized alpha-helices of BCL-2 domains. *Methods Enzymol* **446**, 369-86 (2008).
7. Gavathiotis, E. et al. BAX activation is initiated at a novel interaction site. *Nature* **455**, 1076-81 (2008).
8. Gavathiotis, E., Reyna, D.E., Davis, M.L., Bird, G.H. & Walensky, L.D. BH3-triggered structural reorganization drives the activation of proapoptotic BAX. *Mol Cell* **40**, 481-92 (2010).